Five-axis Strip Machining with Barrel Cutter Based On Tolerance Constraint for Sculptured Surfaces

YaoAn Lu, QingZhen Bi, BaoRui Du, ShuLin Chen, LiMin Zhu, Kai Huang

Abstract—Taking the design tolerance into account, this paper presents a novel efficient approach to generate iso-scallop tool path for five-axis strip machining with a barrel cutter. The cutter location is first determined on the scallop surface instead of the design surface, and then the cutter is adjusted to locate the optimal tool position based on the differential rotation of the tool axis and satisfies the design tolerance simultaneously. The machining strip width and error are calculated with the aid of the grazing curve of the cutter. Based on the proposed tool positioning algorithm, the tool paths are generated by keeping the scallop height formed by adjacent tool paths constant. An example is conducted to confirm the validity of the proposed method.

Keywords—Strip machining, barrel cutter, iso-scallop tool path, sculptured surfaces, differential motion.

I. INTRODUCTION

FIVE-AXIS numerical control (NC) machining is widely used in machining parts with complex surface, such as impellers, blisks and turbine blades. Compared to 3-axis NC machining, the flexibility of five-axis machining could help to avoid interferences and improve both quality of machined surface and machining efficiency.

A lot of papers have been published on tool positioning to increase machining strip width. There are several typical tool positioning methods, such as curvature matching method [1], [2], multi-point machining (MPM) and strip-width maximization machining. The curvature matching method considers the curvatures matching of tool and design surface at the cutter contact (CC) point with local differential geometry. Further, Rao et al. [3]-[5] developed a similar technique called principal axis method (PAM) to machine concave surfaces with an alignment between the principle axis of the cutter and that of the design surface to increase the volume of material removed. Wang et al. [6] presented an algorithm to position the cutter so that its envelope surface and the design surface have the same derivatives up to third order along the direction orthogonal to the cutting direction. Gong et al. [7] proposed a cutter positioning strategy that made the cutter envelope surface have a contact of second-order with the design surface at the CC point. Later, Zhu et al. [8], [9] developed a mathematical model to describe the third-order approximation of the cutter envelope surface. To gain larger machining strip width, Warkentin et al. [10], [11] proposed the MPM method to position the tool at

more than one contact point. Though MPM can generate gouge-free tool positions and increase the machining strip width, it comes at the expense of an extremely complex algorithm. Grap et al. [12] developed the rolling ball method (RBM), which rolled a variable radius ball along the tool path and positioned the tool inside the rolling ball by the principle of the MPM. Later, they developed the arc-intersect method (AIM) to improve the overly conservative property of the RBM [13]. Zhang [14] proposed the concept of strip-width maximization machining to obtain the maximum machining strip width by optimizing the tool position, tool path and tool geometry. Wang et al. [15] suggested a tool positioning method in the flank milling of freeform surfaces using a barrel cutter to obtain the maximum strip width without local gouges.
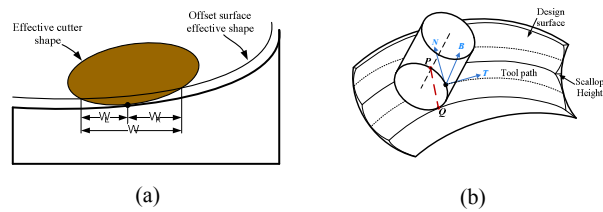

Fig. 1 Machining strip width calculation

Machining strip width is used as a criterion to quality the tool orientation quality in many reported studies. The machining strip width can be easily calculated with flat cutters and torus cutters. Therefore, most work on strip machining so far is focused on those two cutters. As for a barrel cutter, however, the grazing curve of the cutter needs to be calculated first when calculating the machining strip width. Lee et al. [16] used the effective cutting shape of the flat-end tool as shown in Fig. 1 (a), to evaluate the machining strip width. However, the tool swept surface generated by the effective cutting shape of the tool at the various CC points is not the exact swept surface generated by the five-axis tool motion, meaning that the machining strip width evaluated by the effective cutting shape is not accurate [17]. Fard et al. [17] used the swept profile of the cutter and the scallop surface to determine the machining strip width for the flat-end cutter. The machining strip width was defined as the projection of the two intersection points between the swept profile and the scallop surface in the cutting direction, as shown in Fig. 1 (b).

There are several tool path generation methods, such as the iso-parametric, iso-planar, iso-offset, iso-scallop, etc. The iso-scallop approach can generate the least number of tool paths because it can avoid tool path redundancy, having the highest efficiency. Inspired by cutting simulation, Lin et al. [21]

YaoAn Lu, QingZhen Bi, LiMin Zhu and Kai Huang are with the State Key Laboratory of Mechanical System and Vibration, School of Mechanical Engineering, Shanghai Jiao Tong University, Shanghai 200240, P.R. China (corresponding author e-mail: zhulm@sjtu.edu.cn).

BaoRui Du and ShuLin Chen are with the Shenyang Aircraft Corporation, Shenyang 110000, P.R. China.

proposed a generic uniform scallop tool path generation method for five-axis machining. Xu et al. [22] developed a non-redundant tool trajectory generation method for surface finish machining.

In this paper, based on our previous work and the idea of strip-maximization machining, a swept envelope approach to determine the optimal tool orientation for five-axis strip machining with a barrel cutter is presented, then the iso-scallop tool paths on the free-form surface are also generated. The rest of the paper is organized as follows. Section II studies the representation of cutter location (CL) for the barrel cutter. Section III introduces the signed point-to-surface distance function and its differentiability, and then the algorithms for optimizing the tool orientation to maximize the machining strip width and generating the iso-scallop tool paths are proposed. Computer implementations and results are presented in Section IV to confirm the validity of the proposed approach, and conclusions are given in Section V.

II. REPRESENTATION OF CL FOR FIVE-AXIS STRIP MACHINING WITH A BARREL CUTTER

To describe the cutter location during NC machining, a local coordinate frame $o-xyz$ is set up at the designated CC point, as shown in Fig. 2. Its x-axis follows the tangent direction of the CC path. Its z-axis is along the surface normal. Its y-axis is defined by the right-hand rule of the coordinate system. The cutter is represented in a cutter coordinate frame $O_t - x_t y_t z_t$. Its z_t-axis is along the axis of the cutter and x_t-axis lies on the plane determined by the cutter axis and the CC point.
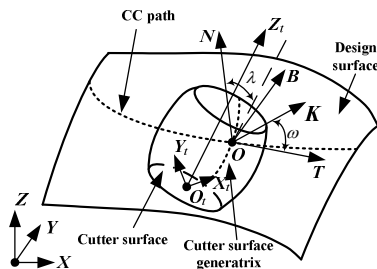

Fig. 2 Cutter coordinate frame and local coordinate frame set up at the CC point

The cutter leads toward the local x-axis with an inclination angle λ, and then rotates about the local z-axis with a tilt angle ω. The rotational transformation from $O_t - x_t y_t z_t$ to $O-xyz$ can be represented as

$$[X_t \quad Y_t \quad Z_t] = [T \quad B \quad N]Q \tag{1}$$

The X_t, Y_t, and Z_t are the unit x, y, and z axes of the cutter coordinate frame. Similarly, the T, B, and N are the unit x, y, and z axes of the local coordinate frame. They are all represented in an inertial frame of reference. Q is a rotational matrix, and has the forms

$$Q = \begin{bmatrix} \cos\omega & -\sin\omega & 0 \\ \sin\omega & \cos\omega & 0 \\ 0 & 0 & 1 \end{bmatrix} \begin{bmatrix} \cos\lambda & 0 & \sin\lambda \\ 0 & 1 & 0 \\ -\sin\lambda & 0 & \cos\lambda \end{bmatrix}$$

$$= \begin{bmatrix} \cos\omega\cos\lambda & -\sin\omega & \cos\omega\sin\lambda \\ \sin\omega\cos\lambda & \cos\omega & \sin\omega\sin\lambda \\ -\sin\lambda & 0 & \cos\lambda \end{bmatrix} \tag{2}$$
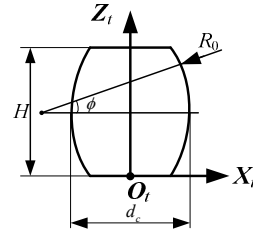
Fig. 3 The generatrix of a barrel cutter

As show in Fig. 3, the generatrix of a barrel cutter surface can be represented as a planar parametric curve $C(\phi)$ in the plane $x_t - z_t$ as(3), where d_c is the maximum diameter of the tool flute, R_0 is the barrel radius, H is the length of tool flute, $\phi \in \left[-\arcsin(H/2R_0), \arcsin(H/2R_0) \right]$,

$$C(\phi) = \begin{bmatrix} x(\phi) \\ y(\phi) \\ z(\phi) \end{bmatrix} = \begin{bmatrix} \dfrac{d_c}{2} - R_0(1-\cos\phi) \\ 0 \\ \dfrac{H}{2} + R_0\sin\phi \end{bmatrix} \tag{3}$$

The section curve of the $x_t - z_t$ plane with the cutter rotary surface is shown in Fig. 4. O is the CC point, N is the unit normal vector at this point, and q is the intersection point of the normal with the axis of the cutter. Obviously, the origin of the frame $O_t - x_t y_t z_t$ can be determined by the following formula

$$O_t = O + aN - bZ_t \tag{4}$$

where a is the distance from O to q, and b is the distance from q to O_t. As discussed above, the angle between the two unit vectors N and Z_t is the inclination angle λ. Hence, we have

$$\tan\lambda = \frac{z'(\phi)}{x'(\phi)} \tag{5}$$

$$\begin{cases} a = \dfrac{x(\phi)}{\sin\lambda} \\ b = z(\phi) + \dfrac{x(\phi)}{\tan\lambda} \end{cases} \tag{6}$$

Fig. 4 Section curve of the $x_t - z_t$ plane with the barrel cutter rotary surface

Given a ϕ, we can calculate an inclination angle λ from (5), then determine a and b according to (6). Therefore, if the CC point $\boldsymbol{O}$, angle ϕ and cutter tilt angle ω are determined, the CL can be represented in the local frame $\boldsymbol{O} - xyz$ as follows

$$\begin{cases} \boldsymbol{O}_t = \boldsymbol{O} - b(\phi)\cos\omega\sin\lambda\boldsymbol{T} - b(\phi)\sin\omega\sin\lambda\boldsymbol{B} + \\ \qquad (a(\phi) - b(\phi)\cos\lambda)\boldsymbol{N} \\ \boldsymbol{Z}_t = \cos\omega\sin\lambda\boldsymbol{T} + \sin\omega\sin\lambda\boldsymbol{B} + \cos\lambda\boldsymbol{N} \end{cases} \quad (7)$$

III. Method for Iso-scallop Tool Path Generation

A. Signed Point-To-Surface Distance Function and Its Differentiability

Given a regular surface $\boldsymbol{S}(u,v)$, and a point $\boldsymbol{p}$, there exists at least one closest point $\boldsymbol{q} \in \boldsymbol{S}(u,v)$, termed as foot point, such that $\|\boldsymbol{p} - \boldsymbol{q}\| = \min_{x \in \boldsymbol{S}(u,v)} \|\boldsymbol{p} - \boldsymbol{x}\|$, where $\|\cdot\|$ stands for the Euclidean norm on $\boldsymbol{R}^3$. If $\boldsymbol{q}$ lies in the interior of $\boldsymbol{S}(u,v)$, then the error vector $\boldsymbol{p} - \boldsymbol{q}$ is normal to $\boldsymbol{S}(u,v)$, i.e., $\boldsymbol{p} - \boldsymbol{q} = \pm d(\boldsymbol{p}) \cdot \boldsymbol{n}^q$, where $\boldsymbol{n}^q$ is the unit outward normal vector of surface $\boldsymbol{S}(u,v)$ at point $\boldsymbol{q}$, as shown in Fig. 5.

Based on the above proposition, we can define the following signed point-to-surface distance function [23].

Definition. If $\boldsymbol{q}$ is unique and lies in the interior of $\boldsymbol{S}(u,v)$, the signed point-to-surface distance function is defined as $d^s(\boldsymbol{p}) = (\boldsymbol{p} - \boldsymbol{q}) \cdot \boldsymbol{n}^q$.

Fig. 5 Signed point-to-surface distance function

Assume the tool axis undergoes a differential rigid body motion $[\boldsymbol{v}, \boldsymbol{\omega}] = [\Delta x, \Delta y, \Delta z, \delta x, \delta y, \delta z]$, where $\boldsymbol{v} = [\Delta x, \Delta y, \Delta z]$ is the differential translation of the tool reference point on the tool

axis, and $\boldsymbol{\omega} = [\delta x, \delta y, \delta z]$ is the differential rotation of the tool axis about the axes of inertial frame of reference, then one has the first-order differential increment of signed point-to-surface distance function

$$\Delta d^s(\boldsymbol{p}) = -\boldsymbol{n}^q \cdot \boldsymbol{v} - (\boldsymbol{q} \times \boldsymbol{n}^q) \cdot \boldsymbol{\omega} \quad (8)$$

For a dense set of data points $\{\boldsymbol{p}_i, 1 \le i \le n\}$ sampled from the grazing curve of the cutter, which satisfy (9) and the u-parameter of their foot points on the design surface are larger than that of the CC point, as the green points shown in Fig. 6,

$$\left| d^s(\boldsymbol{p}_i) \right| \le \varepsilon \quad (9)$$

Fig. 6 Sampled points on the grazing curve of the cutter

where ε is the design tolerance, the tool positioning problem leads to the following minimax problem, or Chebyshev approximation problem

$$\textbf{P1} \qquad \min_{[\boldsymbol{v},\boldsymbol{w}] \in \boldsymbol{R}^6} \max_{1 \le i \le n} \left| d^s(\boldsymbol{p}_i) \right| \qquad (10)$$
$$s.t. \quad -\varepsilon \le d^s(\boldsymbol{p}_i)$$

By introducing one extra variable ξ, problem **P1** can be reformulated as the following differentiable optimization problem

$$\textbf{P2} \qquad \min_{(\boldsymbol{v},\boldsymbol{w},\xi) \in \boldsymbol{R}^7} \xi \qquad (11)$$
$$s.t. \quad -\varepsilon \le d^s(\boldsymbol{p}_i) \le \xi, \quad 1 \le i \le n$$

In problem **P2**, the constraints explicitly require us to reduce the undercut errors and satisfy the design tolerance simultaneously.

Problem **P2** can be solved by sequential linear programming (SLP) method. Solving the linear programming problem to determine the differential motion $[\boldsymbol{v}, \boldsymbol{\omega}]$ of tool axis of each CL on the tool path, the tool reference point becomes $\boldsymbol{O}_t + \boldsymbol{v}$, and the tool axis becomes $\boldsymbol{Z}(t) + \boldsymbol{\omega} \times \boldsymbol{Z}(t)$, it should be noted that the new tool orientation needs to be normalized.

Now, we present the following tool positioning algorithm based on the differential motion of the tool axis for five-axis strip machining.

Algorithm 1 (Tool Positioning Algorithm)

Input: Initial cutter locations along the current tool path; maximum iteration number K; design tolerance ε ;

Output: optimized cutter locations along the tool path

1. Interpolate the tool axes to obtain the tool axis trajectory;
2. For each cutter location along the current tool path, optimize the tool axis using steps 3 to 6;
3. Calculate the grazing curve of the cutter;
4. Obtain the sampled points on the grazing curve by calculating their machining error and foot points on the design surface;
5. Solve the linear programming problem to determine the differential motion $\left[\boldsymbol{v}^k, \boldsymbol{\omega}^k \right]$ of the tool axis;
6. Update the tool reference point and tool orientation;
7. If $k < K$, set $k = k+1$ and go to (1), else exit and report the optimized CLs along the tool path;

B. Algorithm for Iso-scallop Tool Paths Generation

In iso-scallop tool paths, each CL in the next tool path S_{i+1} is calculated from the CL of the current path S_i, so that the scallop height remains the same all over the surface. The newly generated tool path is then used as a master path for generating another tool path.
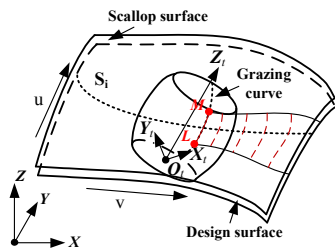
Fig. 7 Intersection with the grazing curve and scallop surface
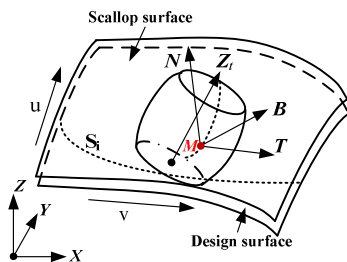
Fig. 8 Local coordinate frame set up at point M

For each CL of the current tool path S_i, the grazing curve of the cutter can be determined based on the tool motion. For the ith CL of the tool path S_i, $\boldsymbol{L}, \boldsymbol{M}$ are the two intersection points between the scallop surface and the grazing curve, as shown in Fig. 7. As mentioned in section 2, a local coordinate can be established at point $\boldsymbol{M}$ on the scallop surface, as shown in Fig. 8. Given ϕ and tilt angle ω , the ith initial CL of the next tool path S_{i+1} can be calculated with (7). After all the initial CLs

along the tool path S_{i+1} are calculated, the grazing curve of each cutter can be determined. Then the cutter locations are adjusted to maximize the machining strip width based on the differential motion of the tool axis.

In order to generate the iso-scallop tool path, the contact point $\boldsymbol{M}$ should remain unchanged, therefore, the differential translation $\boldsymbol{v}$ of the tool axis is set to be zero vector, it means that the sampled points rotate around point $\boldsymbol{M}$. Because the CL is determined on the scallop surface instead of the design surface, the constraint of (9) becomes

$$-\varepsilon \le d^s \left(\boldsymbol{p}_i \right) \le 2\varepsilon \qquad (12)$$

Now, we present the following algorithm for iso-scallop tool path generation for five-axis strip machining with a barrel cutter.

Algorithm 2 (Iso-scallop Tool Path Generation)

Input: The design surface; the geometric parameters of the barrel cutter; ϕ and ω ; the number of CLs on the tool path N; the scallop height or the design tolerance ε .

Output: A set of iso-scallop tool paths $\left\{ S_j \right\}$

1. Generate the first path $S_i (i=1)$ along the iso-parametric curve $u = 0$ of the design surface;
2. For each CL of the current path S_i , calculate the corresponding initial CL on the next tool path S_{i+1} using steps 3 to 4;
3. Calculate the grazing curve of each cutter based on their motion along the current path S_i , and obtain the intersection point $\boldsymbol{M}$ between the grazing curve and the scallop surface;
4. Establish the local coordinate at point $\boldsymbol{M}$ on the scallop surface, and calculate the corresponding initial CL of the next tool path S_{i+1} with ϕ and ω ;
5. Optimize the tool orientation of each CL on the next tool path S_{i+1} with algorithm 1;
6. After obtain the optimized tool path S_{i+1} , calculate the grazing curve of each CL on S_{i+1} , and obtain the intersection points $\boldsymbol{M}_i \left(i = 1, 2, \ldots, N \right)$ between the grazing curves and the scallop surface;
7. If all the intersection points $\boldsymbol{M}_i \left(i = 1, 2, \ldots, N \right)$ of S_{i+1} are outside the parameter range $\left(0 \le u \le 1 \right)$ of the design surface, then STOP, the whole design surface has been covered by the generated tool paths; Else let $i = i+1$ and continue through step 2 for the next new path S_{i+1} .

IV. NUMERICAL IMPLEMENTATION AND SIMULATION

A simulation of five-axis strip machining with a barrel cutter is conducted to demonstrate the validity of the proposed method. The proposed iso-scallop tool path generation method

in this work is implemented in C++ programming language with UG open API. The design free-form surface is shown in Fig. 9 (a). The design tolerance is defined as 0.01mm.

As shown in Fig. 9 (b), the values of R_0, d_c and H are chosen as 15mm, 10mm and 8mm, respectively. Each tool path has thirty CLs. The start tool path curve is on the u=0 boundary curve of the design surface, and the initial CLs of the tool path are determined by (7) with $\phi=0, \omega=\frac{\pi}{2}$, then the tool axis trajectory surface is generated by interpolating thirty pairs of points on these cutter axes with two B-spline curves of degree 3. The grazing curve of each cutter can be calculated with the method proposed in [18]-[20]. After optimizing the tool orientation of each CL on the first tool path with algorithm 1, the next tool path can be calculated with the proposed algorithm 2. Fig. 10 shows the 5-axis tool path distribution generated by the proposed iso-scallop tool path generation method. There are in all 32 tool path curves, and these tool paths are well distributed. The simulation results in Vericut software show that the proposed method is feasible, as illustrated in Fig. 11.
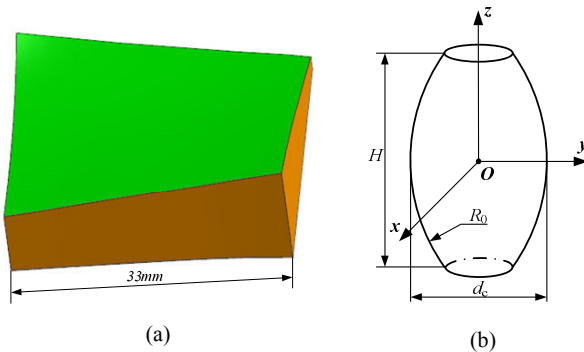
Fig. 9 The design surface and geometry of a barrel cutter
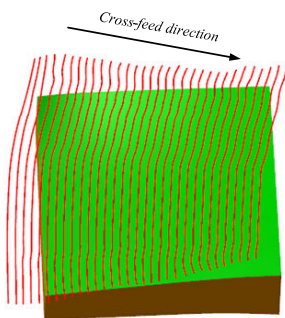
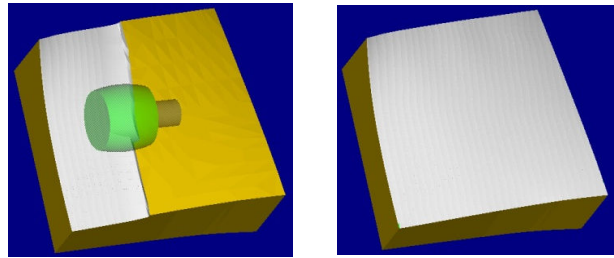Fig. 10 The computational result of Iso-scallop tool paths

Fig. 11 Simulation results in Vericut software

V. CONCLUSION

In this paper, our previous work on signed point-to-surface distance function is extended to develop the model and algorithm for tool path planning for five-axis strip machining. A swept envelope approach to determine the optimal tool orientation for five-axis strip machining with a barrel cutter is proposed in this paper, then the iso-scallop tool paths on free-form surface are generated. The tool orientation is optimized to maximize the machining strip width based on the differential rotation of the tool axis and satisfies the design tolerance simultaneously. Simulation is performed to validate the feasibility of the method.

ACKNOWLEDGMENT

REFERENCES

[1] Mullins S, Jensen C, Anderson D (1993) Scallop elimination based on precise 5-axis tool placement, orientation, and step-over calculations. ASME Adv Des Autom 65:535-544.

[2] Jensen C, Anderson D (1993) Accurate tool placement and orientation for finish surface machining. Journal of Design and Manufacturing 59:127-127

[3] Rao N, Ismail F, Bedi S (1997) Tool path planning for five-axis machining using the principal axis method. International Journal of Machine Tools and Manufacture 37 (7):1025-1040

[4] Bedi S, Gravelle S, Chen Y (1997) Principal curvature alignment technique for machining complex surfaces. Journal of manufacturing science and engineering 119 (4B):756-765

[5] Rao N, Bedi S, Buchal R (1996) Implementation of the principal-axis method for machining of complex surfaces. The International Journal of Advanced Manufacturing Technology 11 (4):249-257

[6] Wang X, Wu X, Li Y (1992) Curvature catering—a new concept for machining sculptured surfaces. Journal of Xi'an Jiaotong University 26 (5):51-58

[7] Gong H, Cao LX, Liu J (2008) Second order approximation of tool envelope surface for 5-axis machining with single point contact. Computer-Aided Design 40 (5):604-615

[8] Zhu LM, Ding H, Xiong YL (2010) Third-order point contact approach for five-axis sculptured surface machining using non-ball-end tools (I): Third-order approximation of tool envelope surface. SCIENCE CHINA Technological Sciences 53 (7):1904-1912

[9] Zhu LM, Ding H, Xiong YL (2010) Third-order point contact approach for five-axis sculptured surface machining using non-ball-end tools (II): Tool positioning strategy. SCIENCE CHINA Technological Sciences 53 (8):2190-2197

[10] Warkentin A, Ismail F, Bedi S (2000) Multi-point tool positioning strategy for 5-axis mashining of sculptured surfaces. Computer Aided Geometric Design 17 (1):83-100

[11] Warkentin A, Ismail F, Bedi S (2000) Comparison between multi-point and other 5-axis tool positioning strategies. International Journal of Machine Tools and Manufacture 40 (2):185-208

[12] Gray P, Bedi S, Ismail F (2003) Rolling ball method for 5-axis surface machining. Computer-Aided Design 35 (4):347-357

[13] Gray PJ, Bedi S, Ismail F (2005) Arc-intersect method for 5-axis tool positioning. Computer-Aided Design 37 (7):663-674

[14] Zhang H (1987) The developing trend of sculptured surface machining in increasing the strip width and decrease the scallop height. Surface Machining and Checking

[15] Wang D, Chen WY, Li T, Xu RF (2009) Five-Axis Flank Milling of Sculptured Surface with Barrel Cutters. Key Engineering Materials 407-408:292-297

[16] Lee YS (1998) Non-isoparametric tool path planning by machining strip evaluation for 5-axis sculptured surface machining. Computer-Aided Design 30 (7):559-570

[17] Fard MJB, Feng H-Y (2009) Effect of tool tilt angle on machining strip width in five-axis flat-end milling of free-form surfaces. The International Journal of Advanced Manufacturing Technology 44 (3-4):211-222

[18] Chiou C-J, Lee Y-S (2002) Swept surface determination for five-axis numerical control machining. International Journal of Machine Tools and Manufacture 42 (14):1497-1507

[19] Chiou JCJ, Lee YS (2005) Optimal tool orientation for five-axis tool-end machining by swept envelope approach. Journal of manufacturing science and engineering 127 (4):810-818

[20] Zhu LM, Zhang XM, Zheng G, Ding H (2009) Analytical expression of the swept surface of a rotary cutter using the envelope theory of sphere congruence. Journal of manufacturing science and engineering 131 (4):0410171-0410177

[21] Lin Z, Fu J, Shen H, Gan W (2014) A generic uniform scallop tool path generation method for five-axis machining of freeform surface. Computer-Aided Design 56:120-132

[22] Xu J, Zhang S, Tan J, Liu X (2012) Non-redundant tool trajectory generation for surface finish machining based on geodesic curvature matching. The International Journal of Advanced Manufacturing Technology 62 (9-12):1169-1178

[23] Zhu LM, Zhang XM, Ding H, Xiong YL (2010) Geometry of signed point-to-surface distance function and its application to surface approximation. Journal of computing and information science in engineering 10 (4):0410031-04100310